Int. J. Advance Soft Compu. Appl, Vol. 12, No. 1, March 2020
ISSN 2074-8523

Automated Detection of *Plasmodium Ovale* and *Malariae* Species on Microscopic Thin Blood Smear Images

Hanung Adi Nugroho, Khonsa Imaroh, Igi Ardiyanto, Zulfanahri, and Eka Legya Frannita

Department of Electrical and Information Engineering,
Faculty of Engineering, Universitas Gadjah Mada, Yogyakarta, Indonesia
e-mail: adinugroho@ugm.ac.id, igi@ugm.ac.id, khonsa.imaroh@mail.ugm.ac.id, zulfanahri@mail.ugm.ac.id, eka.legya.f@mail.ugm.ac.id

Abstract

Malaria is caused by Plasmodium and transmitted by female Anopheles mosquitoes bite. Early detection of malaria has been performed using microscopic thin blood smear images. Even so, in 2014, as many as 321 million times microscopic examination, there were frequent misdiagnosis caused by human factors. Region of Interest (RoI) in image processing is part of the image that has the highest information. The precise determination of the RoI area can make the computer-based identification process work more efficiently, contribute better to the system, and also eliminate objects that are perceived to interfere with the whole process. This study aims to detect parasites by determining the RoI area of two species of Plasmodium Ovale and Plasmodium Malariae. The working principle of detection is using adaptive thresholding, colour segmentation between green channel (G) with hue channel (H) from HSV colour space, and some morphological operation techniques. The data used are digital microscopic images of thin blood smear. This research achieves the sensitivity level of 91.6% and positive predictive value (PPV) of 89.1%. It shows that performance of the proposed parasite detection method is reliable to assist doctor and contributes for developing the computer aided detection in Plasmodium cases.

Keywords: *HSV, Parasite Detection System, Plasmodium Malariae, Plasmodium Ovale, Region of Interest.*

1 Introduction

Malaria is a disease caused by intracellular obligate protozoa of the genus *Plasmodium* and is naturally transmitted by the bite of Anopheles female mosquito [1]. According to World Health Organization (WHO) data, in 2015 there were 212 million malaria cases globally and caused 429,000 deaths worldwide [2]. In Indonesia, there are 85 cases of malaria positive in 100,000 population during 2015 with the highest prevalence on the eastern part of Indonesia [1]. Some malaria cases occur in the northern hemisphere (North America to Europe and Asia). It also often occurs in the southern hemisphere (South America), starting from an area of 2850 m to an area 400 m above sea level. The current status of malaria in the world is estimated to range from 300 to 500 million malaria cases per year and 1.5-2.7 million people are died because of it, especially in African countries [3].

The four main parasite species that because malaria include *Plasmodium Falciparum*, *Plasmodium Ovale*, *Plasmodium Vivax*, and *Plasmodium Malariae*. *Plasmodium Ovale* and *Plasmodium Malariae* are parasite species that have low density levels compared to the other two species, *Plasmodium Vivax* and *Plasmodium Falciparum*, so that identification or even undetectable errors often occur. For that reason, the detection of this parasite requires knowledge and expert skill.

Several studies have been done to diagnose malaria using digital images. However, unlike detection system for *Plasmodium Vivax* and *Plasmodium Falciparum* as recorded in [5]–[9], the detection of *Plasmodium Ovale* and of *Plasmodium Malariae* have not been widely performed [4]. The quality of malaria diagnosis based on microscopic test itself is strongly influenced by the ability, experience and subjectivity of the experts [10], especially for *Plasmodium Ovale* and *Plasmodium Malariae* species. If the detection of these two parasites is not appropriate, it can result in inappropriate medical treatment that leads to cause death. A computer aided diagnosis (CAD) system is needed to support the improvement of diagnosis quality of experts. Initial detection greatly affects the final diagnosis. Therefore, a detection system is made to determine the region of interest of the parasite candidate for malaria identification. Region of interest (RoI) is a part of the image that has the highest information to better contribute to computer-based identification system. Determining a precise RoI area can reduce the unwanted objects that interferes with the entire process in order to provide better detection and diagnostic results especially in *Plasmodium Ovale* and *Plasmodium Malariae* species. The main purpose of this research is to automatically detect *Plasmodium Ovale* and *Plasmodium Malariae* on microscopic thin blood smear digital images.

This paper is arranged as follows. Description of the proposed method and database is described in Section II. Experimental result is given in Section III while section IV explains the discussion. Finally, conclusion part is explained in Section V.

2 Material and Method

The research material used in this study is microscopic thin blood smear digital images of malaria parasites consisting of *Plasmodium Ovale* and *Plasmodium Malariae*. The samples were collected from various regions in Indonesia by parasitologists in Eijkman Molecular Biology Laboratory, RSCM Central Jakarta. The dataset consist of 108 images in which 50 images were categorized as *Plasmodium Ovale* and 58 images were categorized as *Plasmodium Malariae* parasite. Each image has different staining, resolution and illumination. Fig. 1 is a sample used as input on the system.

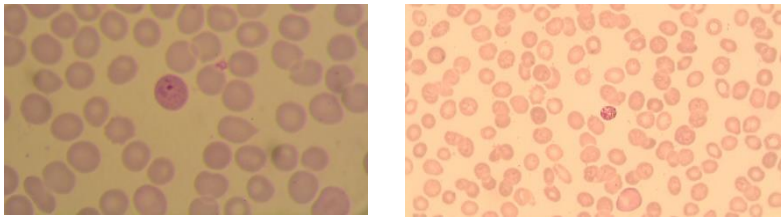

(a) (b)

Fig. 1: Microscopic thin blood smear digital images
(a) *Plasmodium Ovale*, (b) *Plasmodium Malariae*

In Fig. 1, the images of *Plasmodium Ovale* (a) and *Plasmodium Malariae* (b) have characteristic differences. This is due to the different acquisition tools. Image capture uses two different tools but uses the same microscope. Both devices are Nikon D5200 DSLR camera and camera embedded microscope Olympus CX40. Both cameras are connected to one ocular lens microscope with different magnification of 20x and 10x magnification. Image format used in this research is lossless format, bitmap (BMP) with image size of Nikon D5200 camera of 4496 x 3000 and Olympus CX40 microscope of 3264 x 1840.

Fig. 2 shows the proposed method of this study. The proposed method is started with pre-processing step then followed by segmentation and detection step. Pre-processing is conducted by acquisition and normalization, whereas segmentation phases is conducted by using Otsu thresholding method and morphological operation. Moreover, detection phase is conducted by cropping a bounding box area.

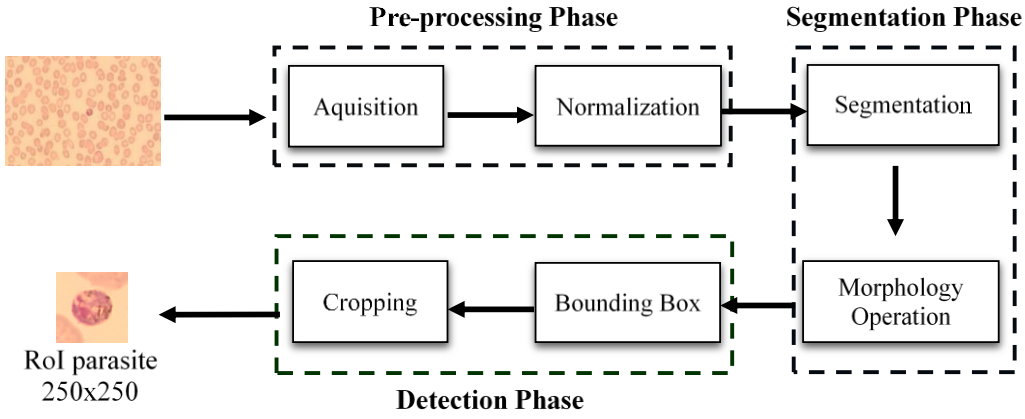

Fig. 2: Block diagram parasite detection method for *Plasmodium Ovale* and *Plasmodium Malariae*

2.1 Pre-processing Phase

The process is started from data acquisition by using two cameras Nikon D5200 DSLR and Olympus CX40 as previously explained. Fig. 1 shows an example of acquired image. The next step is normalization which consists of normalization of image resolution and contrast. Normalization of image resolution is conducted by scaling the image because *Plasmodium Ovale* and *Plasmodium Malariae* images have different resolution.

Improved image quality is needed to improve the quality of perceived image for human vision. Digital images of DSLR camera acquisition results have low quality for further processing. The contrast of the digital image is still low, so the background areas with objects such as parasites and erythrocytes have no clear boundaries. Contrast is the differences between an object with its surrounding indicated by the differences of their pixel values [11]. The contrast quality of an image is judged from the distribution of pixel values on the histogram. In images with good contrast quality, some peaks will be shown based on the total number of objects that appeared in the image. Spreading the distribution of pixel value which results in the wider distance among the peaks can improve the image contrast. One of the common methods to do this technique is contrast stretching. Equation 1 shows mathematical formulation of contrast stretching.

$$o(i,j) = \frac{u(i,j) - c}{d - c}(L - 1) \tag{1}$$

with $o(i,j)$ represents pixel after transformation at *(i,j)*, $u(i,j)$ represents pixel before transformation at *(i,j)*, c represents maximum value from input image and d represents maximum gray level.

In this work, image enhancement is conducted by using contrast stretching. Fig. 3 shows an example of parasite images undergoing contrast stretching.

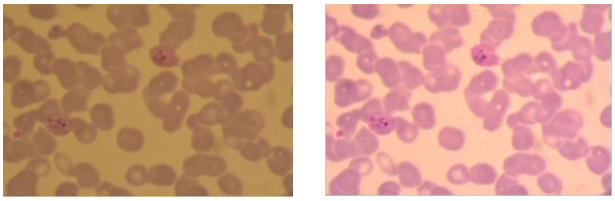

(a) (b)

Fig. 3: Microscopic thin blood smear digital image (a) before and (b) after contrast stretching

2.2 Segmentation Phase

Segmentation aims to separate the parasite area in the image with other objects such as red blood cells, background and other artefacts. This separation is useful to facilitate the detection of parasites to determine the RoI region. Fig. 4 depicts the segmentation process.

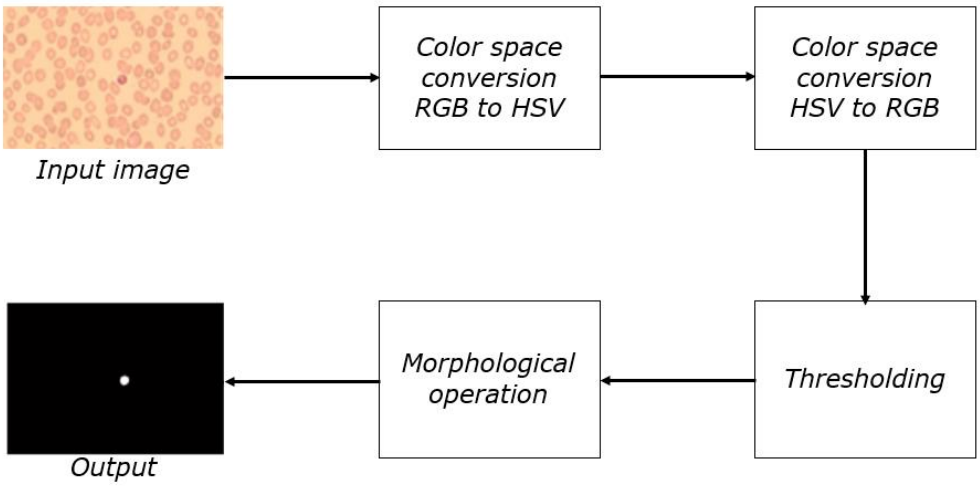

Fig. 4: Segmentation process

2.2.1 Color Space Conversion RGB to HSV

This process is started by converting RGB to HSV to determining the value of H, S and V components. Each of these components has a pixel value of 0/255 to 255/255. Then, HSV conversion is converted to RGB. H value is converted by using rules on Table 1. Here, S and V values are converted to 255/255 if their values are more than 200/255 and are converted to 0 if their values are less than 20/255. Otherwise, S and V values are converted to 128/255.

Table 1: Rules of conversion HSV to RGB of this work

H value	Conversion value	Color
Less than 11/255	0	Red
Less than 32/255	21/255	Orange
Less than 54/255	43/255	Yellow
Less than 116/255	85/255	Green
Less than 141/255	128/255	Cyan
Less than 185/255	170/255	Blue
Less than 202/255	191/255	Violet
Less than 223/255	213/255	Magenta
Less than 244/255	234/255	Pink
0	0	Red

When the HSV image is transformed into RGB image, only the red objects are seen on RGB image so that all the red color and non-red color appears as 1 or white. After that, the image is re-segmented on G channel in RGB color space. This process is intended to convert the red image into grayscale, and then negates it by a subtraction operation of {255-pixels} to produce a negative image. This image is used for next process which is thresholding by Otsu method.

2.2.2 Thresholding

Otsu thresholding method [12] works based on image histogram to determine the optimum thresholding value. It works by maximizing inter-class variance (between-class variance) and is suitable for class statistical discriminant analysis. The histogram shows intensity value frequency of each pixel in one dimension. Thus, the x axis usually denotes a different intensity level whereas the y axis illustrated the number of pixels having the intensity value. Using a histogram, we can group the pixels in the image based on its threshold value. the method aims to determine the threshold value where the total of groups' spreads is at its minimum. If a threshold value is capable in separating groups so that the pixel between groups have different intensity values, then the threshold value is said to be optimal [13].

2.2.3 Morphological Operation

However, thresholding is not enough to get good segmentation results. Improvement of thresholding result is performed by using opening, closing, dilation and erosion operation as explained in Equation 2 to 5 [14][15],

$$A_B = (A \ominus B) \oplus B \tag{2}$$

$$A^B = (A \oplus B) \ominus B \tag{3}$$

$$A \oplus B = \{z | (\hat{B})_Z \cap A \neq \emptyset\} \tag{4}$$

$$A \ominus B = \{z | (\hat{B})_Z \subseteq A\} \tag{5}$$

with *A* indicates the input images and *B* is structuring element.

2.3 Detection Phase

The detection phase consists of two main processes. The first process is determination of the bounding box on the segmented image and the second is determination of RoI image on the normalized image. The output of this phase is RoI image consisting of identified candidate parasite cells. When bounding boxes are formed on the segmented image, the cropping is then conducted based on the bounding box on the normalized image. Several RoI images are obtained as a result of detection process as shown in Fig. 5.

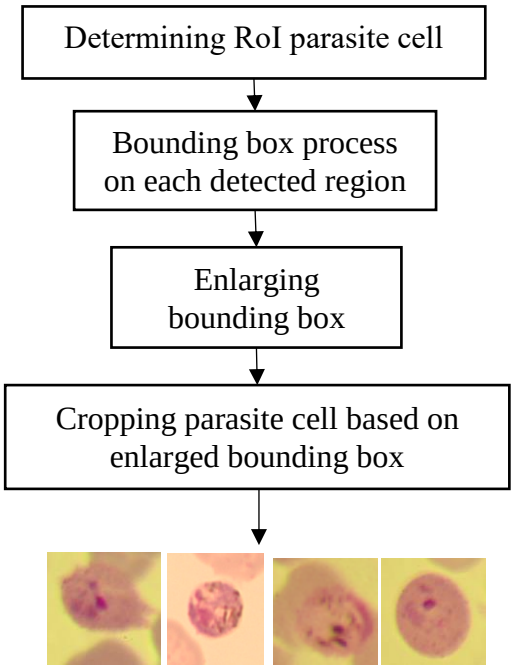

Fig. 5: Detection process

2.4 Validation Method

The performance evaluation is conducted by using two parameters, i.e. sensitivity rate and predicted positive value (PPV) which are calculated using Equation (6) and (7).

$$Sensitivity = \frac{TP}{TP + FN} \times 100\% \quad (6)$$

$$PPV = \frac{TP}{TP + FP} \times 100\% \quad (7)$$

Here, TP defines the true positive rate, whereas FP is false positive rate and FN illustrates the number of false negative rate.

3 Result and Discussion

The automated parasite detection method for *Plasmodium Ovale* and *Plasmodium Malariae* has been proposed. The result on each phase is presented as follows.

3.1 Pre-processing Result

3.1.1 Normalization of Image Size

The normalization process is often called as image resizing. To find out how many resizing scales between the two types of images, the area of erythrocytes of each image is calculated. This process requires about 15 erythrocytes of normal size for each image. Table 2 shows the scale size result.

Table 2: Erythrocytes area comparison between *Plasmodium Ovale* and *Plasmodium Malariae*

Average of erythrocytes area on 15 images (pixel)		Scale
Plasmodium Ovale	*Plasmodium Malariae*	
29,134	13,839	0.475

Based on Table 1 the average of erythrocytes area in the *Plasmodium Ovale* image is greater than the average area of *Plasmodium Malariae* image erythrocytes. Hence, the resizing process is performed on the *Plasmodium Ovale* image 0.475 times that of *Plasmodium Malariae*. The obtained resolution for *Plasmodium Ovale* after resizing is 1855x1238.

3.1.2 Normalization of Image Size

Fig. 6 shows the result of contrast stretching on several *Plasmodium Ovale* microscopic images.

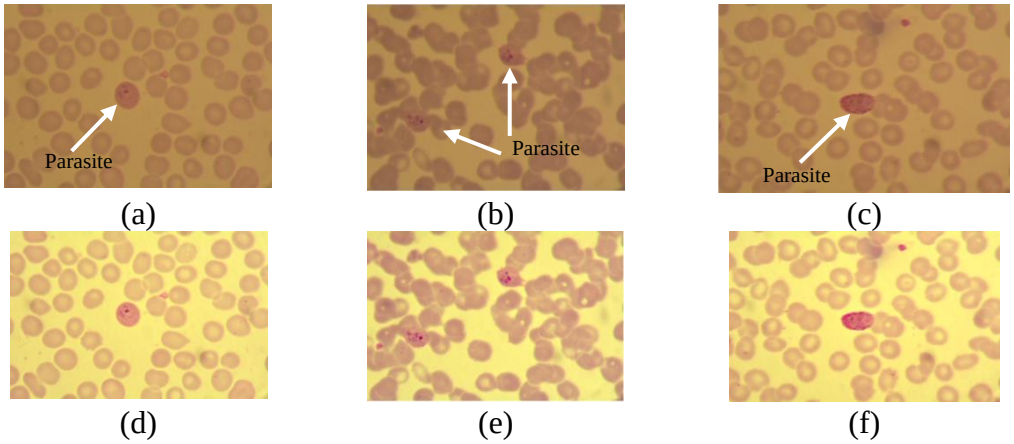

Fig. 4: Microscopic thin blood smear digital images of *Plasmodium Ovale* (a), (b), (c) original images, (d), (e), (f) images after contrast stretching

As shown in Fig. 6, normalization process by using contrast stretching method successfully improves the quality of initial image. The contrast stretching results are more clearly than the initial image. The parasite candidates are also recognizable.

3.2 Segmentation

As explained in Fig. 4, the segmentation process primarily uses the HSV color space which is divided into three channels, i.e. H, S and V. The following segmentation results of both parasites are described in Fig. 7.

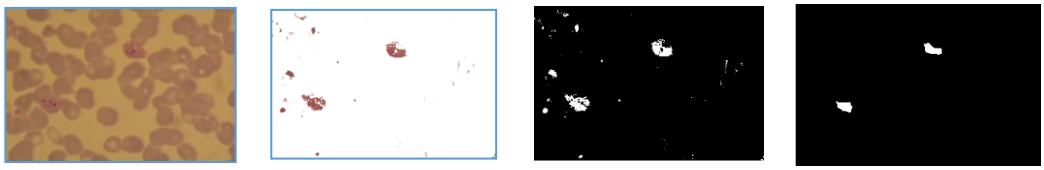

(a) (b) (c) (d)

Fig. 7: The result of segmentation process. (a) origin image, (b) HSV conversion, (c) thresholded image, (d) morphological operation result

3.3 Detection Phase

Binary image which shows the parasite cell is the result of segmentation phase as seen in Fig. 7(d). The parasite cell needs to be marked by bounding box process. Since HSV segmentation images are used to amplify the nuclear region and to weaken other parts so that the initial result of parasite cell bounding box only covers the majority of the nucleus region as seen in Fig. 8(c). Therefore, the initial bounding box needs to be zoomed to cover all areas of the parasite cell by adding a bounding box size of k pixels as seen in Fig. 8 (d). The value of k represents the average width of the cytoplasm of the parasite cell.

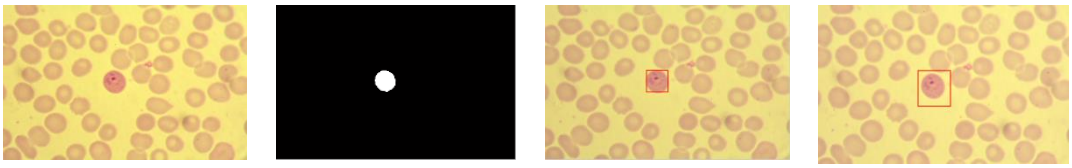

(a) (b) (c) (d)

Fig. 8: Bounding box on RoI parasite cell (a) initial image, (b) segmentation result, (c) bounding box initial, (d) zoomed image

Cropping the RoI parasite cell is conducted based on the bounding box result. Fig. 9 shows the result of cropping process from Fig. 8 (d). The cropped images are stored in the dataset which can be used for phase identification and classification. All results of detection process are summarized in Fig. 10.

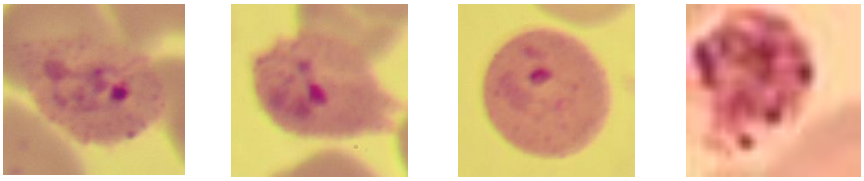

Fig. 9: Result of cropping parasite cell images

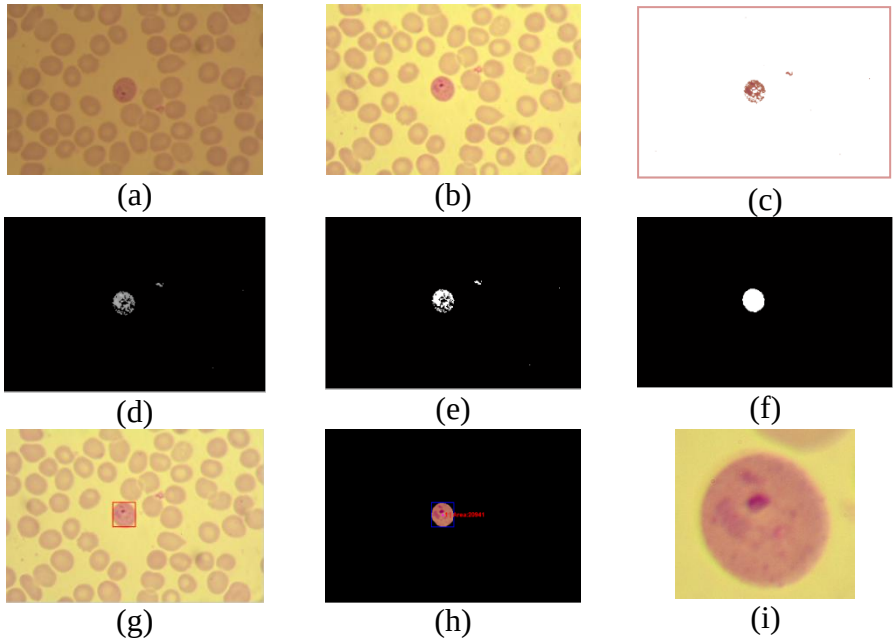

(a) (b) (c)

(d) (e) (f)

(g) (h) (i)

Fig. 10: Result of parasite detection: (a) original image, (b) contrast stretching, (c) HSV segmentation color, (d) canal G on RGB, (e) thresholding, (f) morphological operation, (g) bounding box (h) calculating area and (i) cropped image (RoI)

3.4 Validation

The results are validated by using sensitivity and PPV to determine the proposed method performance. The number of true positive, false positive and false negative is shown in Table 3, while the validation result is summarized in Table 4.

Table 3. Calculation of TP, FP, and FN

Data	Result
True positive	98
False positive	12
False negative	9

Table 4. Performance of proposed method

Data	Result
Sensitivity	91.6%
PPV	89.1%

Table 5. Validation data of (a) *Plasmodium Ovale* and (b) *Plasmodium Malariae*

Plasmodium Ovale			*Plasmodium Malariae*		
Data	Number of infected cells	Number of detected cells	Data	Number of infected cells	Number of detected cells
Image 1	1	1	Image 1	1	1
Image 2	2	2	Image 2	1	1
Image 3	1	1	Image 3	1	1
Image 4	2	2	Image 4	1	1
Image 5	1	1	Image 5	1	1
Image 6	1	1	Image 6	1	2
Image 7	1	1	Image 7	1	1
Image 8	1	1	Image 8	1	1
Image 9	1	1	Image 9	1	1
Image 10	1	1	Image 10	1	1
Image 11	1	1	Image 11	1	1
Image 12	1	1	Image 12	1	1
Image 13	1	1	Image 13	1	1
Image 14	2	2	Image 14	1	0
Image 15	1	1	Image 15	1	1
Image 16	1	1	Image 16	1	0
Image 17	1	1	Image 17	1	1
Image 18	1	1	Image 18	1	1
Image 19	1	1	Image 19	1	1
Image 20	1	1	Image 20	1	2
Image 21	1	1	Image 21	0	0
Image 22	1	1	Image 22	0	0
Image 23	1	1	Image 23	0	1
Image 24	1	1	Image 24	0	0
Image 25	1	1	Image 25	1	0
Image 26	1	1	Image 26	1	1
Image 27	1	1	Image 27	1	2
Image 28	1	1	Image 28	1	1
Image 29	1	1	Image 29	1	1
Image 30	1	1	Image 30	1	1
Image 31	1	1	Image 31	1	1
Image 32	1	1	Image 32	1	2
Image 33	1	2	Image 33	1	1
Image 34	1	2	Image 34	1	1
Image 35	1	1	Image 35	1	1
Image 36	1	0	Image 36	1	1
Image 37	1	1	Image 37	1	1
Image 38	1	1	Image 38	1	1
Image 39	1	0	Image 39	1	2
Image 40	1	1	Image 40	1	2
Image 41	1	1	Image 41	1	2
Image 42	1	1	Image 42	1	1
Image 43	1	3	Image 43	1	1
Image 44	1	1	Image 44	1	1
Image 45	1	1	Image 45	1	1
Image 46	1	1	Image 46	1	1
Image 47	1	1	Image 47	1	1
Image 48	1	0	Image 48	1	1
Image 49	1	1	Image 49	1	1
Image 50	1	1	Image 50	1	1
Image 51	1	0			
Image 52	1	1			
Image 53	1	1			
Image 54	1	0			
Image 55	1	1			
Image 56	1	0			
Image 57	1	1			
Image 58	1	1			
Total	**61**	**59**	**Total**	**46**	**51**

In addition, the detail of the validation result obtained from each image is shown in Table 5. Based on the aforementioned tables, sensitivity and PPV results obtained from the detection of each image are 91.6% and 89.1%, respectively. These results show that the proposed method is suitable for detection of *Plasmodium Ovale* and *Plasmodium Malariae* parasites.

4 Conclusion

An automated parasite detection of *Plasmodium Ovale* and *Plasmodium Malariae* has been developed. The proposed method uses combination of adaptive thresholding, colour segmentation between green channel (G) with hue channel (H) from HSV colour space, some morphological operation techniques and bounding box. The proposed method successfully obtains sensitivity of 91.6% and positive predictive value (PPV) of 89.1%. These results indicate that the proposed method is reliable to assist doctor in detecting *Plasmodium Ovale* and *Plasmodium Malariae* parasites for support decision making. Moreover, the RoI results are useful to be processed further in developing classification method for each phase of *Plasmodium Ovale* and *Plasmodium Malariae* parasites.

ACKNOWLEDGEMENTS
This work is funded by the Directorate General of Higher Education, Ministry of Research, Technology and Higher Education, Republic of Indonesia. The authors would like to thanks to Eijkman Molecular Biology Laboratory, RSCM Central Jakarta for providing the dataset. The authors would also like to thank the anonymous reviewers for encouraging reviews and suggestions.

References

[1] InfoDatin Malaria. (2016). *Pusat Data dan Informasi Kementerian Kesehatan RI*, pp. 1–7.

[2] World Malaria Report. (2016). *World Health Organization*, Geneva.

[3] Arsin, A. A. (2012). Malaria di Indonesia. *MASAGENA PRESS*, Makassar.

[4] Li, P., Zhao, Z., Xing, H., Li, W., Zhu, X., Cao, Y., ... & Cui, L. (2016). Plasmodium malariae and Plasmodium ovale infections in the China–Myanmar border area. *Malaria journal*, 15(1), 557.

[5] Peñas, K. E. D., Rivera, P. T., & Naval, P. C. (2017, July). Malaria parasite detection and species identification on thin blood smears using a

convolutional neural network. In *2017 IEEE/ACM International Conference on Connected Health: Applications, Systems and Engineering Technologies (CHASE)* (pp. 1-6). IEEE.

[6] Ghosh, M., Das, D., Chakraborty, C., & Ray, A. K. (2011, November). Plasmodium vivax segmentation using modified fuzzy divergence. In *2011 International Conference on Image Information Processing* (pp. 1-5). IEEE.

[7] Nugroho, H. A., Saputra, W. A., Permanasari, A. E., & Murhandarwati, E. E. H. (2017, August). Automated determination of Plasmodium region of interest on thin blood smear images. In *2017 International Seminar on Intelligent Technology and Its Applications (ISITIA)* (pp. 352-355). IEEE.

[8] Pattanaik, P. A., Swarnkar, T., & Sheet, D. (2017, November). Object detection technique for malaria parasite in thin blood smear images. In *2017 IEEE International Conference on Bioinformatics and Biomedicine (BIBM)* (pp. 2120-2123). IEEE.

[9] Preedanan, W., Phothisonothai, M., Senavongse, W., & Tantisatirapong, S. (2016, February). Automated detection of plasmodium falciparum from Giemsa-stained thin blood films. In *2016 8th International Conference on Knowledge and Smart Technology (KST)* (pp. 215-218). IEEE.

[10] Saputra, W. A., Nugroho, H. A., & Permanasari, A. E. (2016, October). Toward development of automated plasmodium detection for Malaria diagnosis in thin blood smear image: An overview. In *2016 International Conference on Information Technology Systems and Innovation (ICITSI)* (pp. 1-6). IEEE.

[11] Maysanjaya, I. M. D. (2016). *Identifikasi Fase Plasmodium Vivax pada Citra Mikroskopis Digital Sediaan Darah Tipis* (Master Thesis, Universitas Gadjah Mada).

[12] Maysanjaya, I. M. D., Nugroho, H. A., Setiawan, N. A., & Murhandarwati, E. E. H. (2016). Segmentation of Plasmodium vivax phase on digital microscopic images of thin blood films using colour channel combination and Otsu method. AIP Conference Proceedings, 1755(1), 160002. doi:10.1063/1.4958595

[13] Lee, H., & Park, R. H. (1990). Comments on" An optimal multiple threshold scheme for image segmentation. *IEEE Transactions on systems, man, and cybernetics*, 20(3), 741-742.

[14] Gonzalez, R. C., & Woods, R. E. (2006). Digital Image Processing (3rd Edition). Upper Saddle River, NJ, USA: Prentice-Hall, Inc.

[15] Arco, J. E., Górriz, J. M., Ramírez, J., Álvarez, I., & Puntonet, C. G. (2015). Digital image analysis for automatic enumeration of malaria parasites using morphological operations. Expert Systems with Applications, 42(6), 3041-3047. doi:https://doi.org/10.1016/j.eswa.2014.11.037.